Molecular evidence for dual pyrethroid-receptor sites on a mosquito sodium channel

Yuzhe Du[a,1], Yoshiko Nomura[a,1], Gul Satar[a], Zhaonong Hu[a], Ralf Nauen[b], Sheng Yang He[c,d], Boris S. Zhorov[e,f], and Ke Dong[a,2]

[a]Department of Entomology, Genetics and Neuroscience Programs, [c]Department of Energy Plant Research Laboratory, and [d]Howard Hughes Medical Institute, Michigan State University, East Lansing, MI 48824; [b]Bayer CropScience, D-40789 Monheim, Germany; [e]Department of Biochemistry and Biomedical Sciences, McMaster University, Hamilton, ON, Canada L8S 4K1; and [f]Sechenov Institute of Evolutionary Physiology and Biochemistry, Russian Academy of Sciences, St. Petersburg 194223, Russia

Edited by Janet Hemingway, Liverpool School of Tropical Medicine, Liverpool, United Kingdom, and approved May 22, 2013 (received for review March 26, 2013)

Pyrethroid insecticides are widely used as one of the most effective control measures in the global fight against agricultural arthropod pests and mosquito-borne diseases, including malaria and dengue. They exert toxic effects by altering the function of voltage-gated sodium channels, which are essential for proper electrical signaling in the nervous system. A major threat to the sustained use of pyrethroids for vector control is the emergence of mosquito resistance to pyrethroids worldwide. Here, we report the successful expression of a sodium channel, AaNa$_v$1–1, from *Aedes aegypti* in *Xenopus* oocytes, and the functional examination of nine sodium channel mutations that are associated with pyrethroid resistance in various *Ae. aegypti* and *Anopheles gambiae* populations around the world. Our analysis shows that five of the nine mutations reduce AaNa$_v$1–1 sensitivity to pyrethroids. Computer modeling and further mutational analysis revealed a surprising finding: Although two of the five confirmed mutations map to a previously proposed pyrethroid-receptor site in the house fly sodium channel, the other three mutations are mapped to a second receptor site. Discovery of this second putative receptor site provides a dual-receptor paradigm that could explain much of the molecular mechanisms of pyrethroid action and resistance as well as the high selectivity of pyrethroids on insect vs. mammalian sodium channels. Results from this study could impact future prediction and monitoring of pyrethroid resistance in mosquitoes and other arthropod pests and disease vectors.

Pyrethroids are a large class of synthetic analogs of natural pyrethrins from the flowers of the pyrethrum daisy (*Tanacetum cinerariaefolium*) (1). They have been used extensively for the control of insect pests and disease vectors for more than three decades. In addition to conventional indoor residue sprays (IRS), use of insecticide-treated nets (ITNs) and long-lasting insecticide-treated nets (LLINs) has been proven to be effective against a wide range of insect vectors involved in the transmission of human diseases, such as malaria, leishmaniasis, Chagas disease, and dengue (2). Currently, ITNs and LLINs are some of the most powerful control measures to reduce malaria morbidity and mortality worldwide. To date, pyrethroids are the only insecticides used for net impregnation in both ITNs and LLIN because of their fast-acting and highly insecticidal activities and their low mammalian toxicity (2, 3).

Voltage-gated sodium channels are essential for the initiation and propagation of action potentials in the nervous system and other excitable cells. Like mammalian sodium channels, insect sodium channels comprise four homologous domains (I–IV), each having six membrane spanning segments (S1–S6) (Fig. 1). S4 segments along with S1–S3 segments constitute the voltage-sensing modules, whereas S5, S6, and the membrane-reentrant loop (called the P-region), which connects S5 and S6 segments, form the pore module. In response to membrane depolarization, S4 segments move outward, initiating the opening of sodium channels (i.e., the opening of the activation gate). This process is called activation. According to the crystal structures of the closed potassium channels (4, 5) and the bacterial voltage-gated sodium channel (Na_VAb) (6), the activation gate is located at the cytoplasmic end of the pore, where all four S6 segments converge. After a brief opening, the sodium channel is inactivated. This is achieved by the movement of an inactivation particle (formed mainly by residues in the short intracellular linker connecting domains III and IV), which physically occludes the open pore. Upon repolarization, the sodium channel recovers from the fast inactivation and deactivates (i.e., closing of the activation gate). Pyrethroids mainly inhibit channel deactivation and inactivation, resulting in prolonged opening of sodium channels (7–10). As a consequence, pyrethroids cause repetitive firing and depolarization of the nerve membrane, disrupting the electrical signaling in the insect nervous system (7–9).

As highlighted recently (11), a major threat to the sustained use of pyrethroids in malaria control is the development of pyrethroid resistance. Indeed, pyrethroid resistance has emerged as one of the most serious concerns to future success of malaria control (references in ref. 12). A prominent mechanism of pyrethroid resistance is called knockdown resistance (kdr), which is caused by mutations in the sodium channel and has been documented globally in almost all major arthropod pests and disease vectors (12–14). To date, more than a dozen kdr mutations have been confirmed to reduce insect sodium channel sensitivity to pyrethroids using the *Xenopus* oocyte expression system (12–14). Identification of kdr mutations has already led to successful development of rapid and accurate molecular methods to detect pyrethroid resistance in field populations, particularly in various mosquito populations (references in ref. 12).

Identification of kdr mutations has also set a foundation for computer modeling and model-guided mutagenesis to address a fundamental question in pyrethroid action and pyrethroid resistance: the elusive pyrethroid-receptor site(s) on the sodium channel. In a previous study, O'Reilly et al. proposed a pyrethroid-receptor site model in the open state of the house fly sodium channel, based on the crystal structure of voltage-gated potassium channels (15). This model predicts that pyrethroids bind to the lipid-exposed interface formed by the linker helix connecting S4 and S5 in domain II (IIL45), and helices IIIS6 and IIS5 (the IIL45–IIS5–IIIS6 triangle model or site 1 hereinafter). Experimental data from systematic site-directed mutagenesis

Author contributions: Y.D., S.Y.H., B.S.Z., and K.D. designed research; Y.D., Y.N., G.S., and Z.H. performed research; R.N. contributed new reagents; Y.D., Y.N., B.S.Z., and K.D. analyzed data; and Y.D., S.Y.H., B.S.Z., and K.D. wrote the paper.

The authors declare no conflict of interest.

This article is a PNAS Direct Submission.

Data deposition: The sequences reported in this paper have been deposited in the GenBank database (accession no. KC107440).

[1]Y.D. and Y.N. contributed equally to this work.

[2]To whom correspondence should be addressed. E-mail: dongk@msu.edu.

This article contains supporting information online at www.pnas.org/lookup/suppl/doi:10.1073/pnas.1305118110/-/DCSupplemental.

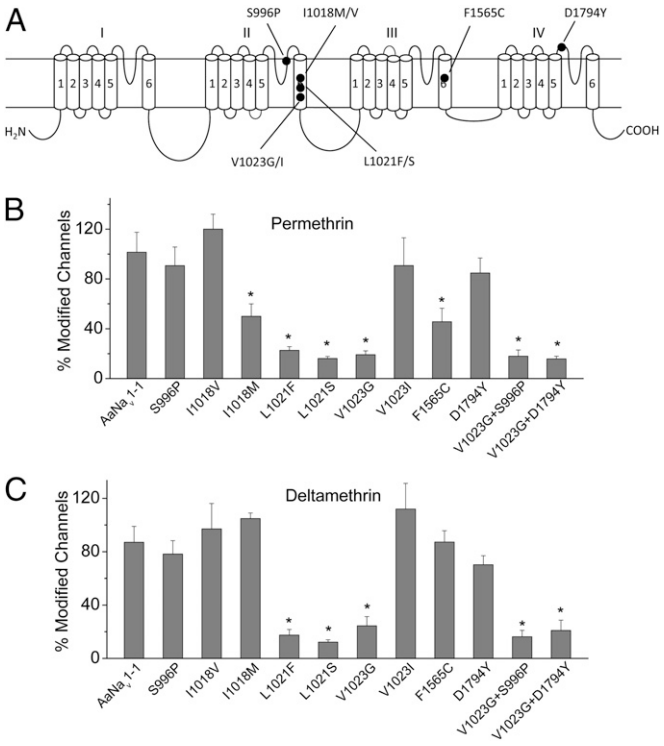

Fig. 1. Five pyrethroid-resistance–associated mutations reduce the sensitivity of the AaNa$_v$1–1 sodium channel to pyrethroids. (*A*) Topology of the AaNa$_v$1–1 channel protein illustrating pyrethroid-resistance–associated mutations (solid circles) identified in *Aedes aegypti* populations around the world and two pyrethroid-resistance–associated mutations identified in *Anopheles* and *Culex* species. Sodium channels are large transmembrane proteins with four homologous repeats (I–IV), each having six transmembrane segments (1–6). The mutations are numbered according to amino acid positions in the AaNa$_v$ protein (GenBank accession no. EU399181). S996P, I1018V/M, and V1023G/I correspond to S989P, I1011V/M, and V1016G/I of the house fly sodium channel. (*B* and *C*) Channel sensitivity to permethrin (1 μM) (*B*) and deltamethrin (1 μM) (*C*). Percentage of channel modification by pyrethroids was determined by the method developed by Tatebayashi et al. (31). The number of oocytes for each mutant construct was >5. Error bars indicate mean ± SEM. Asterisks indicate significant differences from the AaNa$_v$1–1 channel as determined by using one-way analysis of variance with Scheffé's post hoc analysis, and significant values were set at $P < 0.05$.

studies in these regions support this model (16, 17). Several key kd mutations in IIL45, IIS5, and IIIS6 are predicted to confer resistance by altering pyrethroid binding (18, 19). However, this model cannot accommodate mutations detected in other regions of the sodium channel, including the L1021F mutation in IIS6 of the mosquito sodium channel. Analogous mutations, e.g., L1014F in the housefly sodium channel and L993F in the cockroach sodium channel are one of the most widespread pyrethroid-resistance mutations in diverse pest species (14, 20). Furthermore, new sodium channel mutations associated with pyrethroid resistance continue to emerge in various arthropod pests, particularly in disease vectors (12). For example, as many as seven new pyrethroid-resistance–associated sodium channel mutations (Fig. 1*A*) have been reported in *Aedes aegypti* populations collected from Africa, Asia, and Latin America (12) and, more recently, several new sodium channel mutations are identified to be associated with pyrethroid resistance in *Anopheles gambiae* (21) and *Culex quinquefasciatus* (22, 23). Interestingly, many of these mutations are not located in predicted site 1 (i.e., the IIL45–IIS5–IIIS6 triangle) and their role in conferring pyrethroid resistance remains to be demonstrated experimentally.

None of pyrethroid-resistance–associated mutations detected in mosquito species has been functionally characterized in mosquito sodium channels due to the lack of a functional expression system for mosquito sodium channels. Several years ago, we initiated an effort to study the molecular action of pyrethroids and pyrethroid resistance in mosquitoes. In this paper, we report the successful expression of the *Ae. aegypti* sodium channel AaNa$_v$1–1 in *Xenopus* oocytes. Establishment of this expression system enabled us to systematically characterize pyrethroid-resistance–associated mutations coupled with computer modeling, which led to the discovery of a second putative pyrethroid-receptor site on mosquito sodium channels.

Results and Discussion

Expression and Functional Characterization of a Mosquito Sodium Channel in *Xenopus* Oocytes. A full-length sodium channel cDNA clone, *AaNa$_v$1–1*, was isolated from adults of *Ae. aegypti*. An initial attempt to express *AaNa$_v$1–1* in *Xenopus* oocytes, however, produced only small sodium currents. It is known that robust expression of the *Drosophila melanogaster* sodium channel requires an auxiliary subunit protein temperature-induced paralytic E (TipE) (24, 25). We cloned a *TipE*-like cDNA, *AaTipE*, from *Ae. aegypti* and used it for coexpression with the *AaNav1-1* cRNA (1:1 ratio) in *Xenopus* oocytes. Indeed, *AaTipE* significantly increased the amplitude of AaNa$_v$1–1 sodium currents (Fig. S1*B*). The voltage dependences of activation and steady-state inactivation (Fig. S1*C*) are similar to those of sodium channels from other insects (25–28).

One major feature of pyrethroid action on sodium channels is the induction of a slowly decaying tail current upon termination of depolarizing pulse (i.e., deactivation following repolarization of the membrane) in voltage-clamp experiments (29). Because pyrethroids preferably interact with the open state of insect sodium channels (19), to elicit large pyrethroid-induced tail currents, we applied a 100-pulse train of 5-ms depolarization from −120 to 0 mV, with a 5-ms interval. Pyrethroids are classified either as type I or type II based on their chemical structures, poisoning symptoms, and effects on the nervous system (29, 30). Compared with type I pyrethroids, such as permethrin (PMT), type II pyrethroids including deltamethrin (DMT) generally modify sodium channel gating more dramatically, causing a much more slowly decaying tail current during deactivation upon repolarization (19). This was also the case for the AaNa$_v$1–1 channel (Fig. S1 *D* and *E*). The resulting pyrethroid-induced tail currents serve as a measure of channel sensitivity to pyrethroids (31).

Five Mutations Confer the AaNa$_v$1–1 Channel Resistance to Pyrethroid Insecticides. The establishment of a functional expression system for the AaNa$_v$1–1 channel enabled us to examine whether any of the seven pyrethroid-resistance–associated mutations found in *Ae. aegypti* (Fig. 1*A*) affect pyrethroid sensitivity of a native sodium channel. In addition, we also examined two mutations, leucine (L) to phenylalanine (F) or serine (S) mutation at amino acid position 1021 (L1021F/S) in domain II segment 6 (IIS6) because they were found in pyrethroid-resistant *Anopheles* and *Culex* mosquitoes (12). The L1021F mutation corresponds to L1014F in the house fly sodium channel and L993F in the cockroach sodium channel, both of which have previously been shown to reduce the sensitivity of respective sodium channels to pyrethroids (12, 14), whereas the L1021S mutation reduces the sensitivity of a *Drosophila* sodium channel to pyrethroids (32). Because S996P and D1794Y mutations are often found to coexist with V1023G in pyrethroid-resistant field populations of *Ae. Aegypti* (references in ref. 12), we also examined the effects of two double mutations. Accordingly, a total of nine single mutant and two double mutant AaNa$_v$1–1 channels were constructed. All mutants generated sufficient sodium currents in *Xenopus* oocytes for further functional analysis. None of mutations

altered the voltage dependences of activation and inactivation (Table S1).

To evaluate channel sensitivity to PMT and DMT, the percentage of sodium channels modified by pyrethroids was determined by quantifying the amplitude of pyrethroid-induced tail current (Fig. S1 *D* and *E*) (31). As shown in Fig. 1 *B* and *C*, of the six mutations located in IIS6, V1023G, L1021F, and L1021S mutations reduced $AaNa_v1$–1 channel sensitivity to both pyrethroids, whereas I1018M reduced $AaNa_v1$–1 channel sensitivity to PMT, but not to DTM. In contrast, I1018V and V1023I did not alter channel sensitivity to either pyrethroid (Fig. 1 *B* and *C*). Of the remaining three mutations, F1565C in IIIS6 reduced the sensitivity of the $AaNa_v1$–1 channel to PMT, but not to DMT (Fig. 1 *B* and *C*). This is in agreement with our earlier findings that this mutation reduces the sensitivity of cockroach sodium channels to type I, but not type II, pyrethroids (33). In addition, neither V1023G/S996P nor V1023G/D1794Y was more resistant to pyrethroids than the single mutants (Fig. 1 *B* and *C*). Altogether, our functional analysis using the $AaNa_v1$–1 channel provides direct evidence for the involvement of three *Ae. aegypti* mutations (I1018M, V1023G in IIS6, and F1565C in IIIS6) and also two *Anopheles*/*Culex* mutations (L1021F/S in IIS6) in $AaNa_v1$-1 channel insensitivity to pyrethroids. Furthermore, it is worth mentioning that although S996P and D1794Y mutations were concurrent with V1023G in pyrethroid-resistant field populations of *Ae. Aegypti*, neither of them imposes additive or synergistic effects on the V1023G-mediated pyrethroid resistance.

Molecular Mapping of a Second Pyrethroid-Receptor Site on the $AaNa_v1$–1 Channel. Two *Ae. aegypti* kdr mutations confirmed in this study, V1023G in IIS6 and F1565C in IIIS6, are located in the previously identified receptor site (site 1) (Fig. S2). Surprisingly, the other three kdr mutations, I1018M, L1021F, and L1021S, are not close to site 1 (Fig. S2). Importantly, kdr mutations at L1021 (corresponding to L1014 and L993 in the house fly and cockroach sodium channels, respectively) are widespread in diverse pyrethroid-resistant populations of many pest species (14, 20), and the L993F mutation in the cockroach sodium channel has been shown to reduce pyrethroid binding using Schild analysis (18). These findings raise the possibility that site 1 may not be the only pyrethroid-receptor site on insect sodium channels, as was previously proposed by Vais et al. based on Hill plot analysis (19). Their work suggested that the M918T mutation in IIL45 (within site 1) in the *Drosophila* sodium channel reduces the number of apparent pyrethroid-binding sites per channel from two to one (19). However, the molecular identity of this putative second site remained elusive.

To explore the molecular identity of a second pyrethroid-receptor site on the $AaNa_v1$–1 channel, we have built a homology model of the inner-pore region of the $AaNa_v1$–1 channel using the X-ray structure of the potassium channel $K_v1.2$ (34). From here on, we replaced the sequence-based amino acid numbering with a nomenclature that is universal for sodium channels and other P-loop ion channels (35). This nomenclature, which is described in Fig. 2 legend, permits recognition of symmetric positions of amino acid residues in the four homologous domains within the same channel and also comparison with sodium channels from other species (Fig. 2*A*). When necessary, we also show the sequence-based residue number in parentheses. According to our model, the three mosquito kdr mutations, $I^{2i13(1018)}M$ and $L^{2i16(1021)}F/S$, are located in the I/II domain interface outside of site 1, whereas the kdr mutation $F^{3i13(1565)}C$ and a previously identified pyrethroid-sensing residue, $F^{3i16(1518)}$, in the cockroach sodium channel (16) are situated in the II/III domain interface within site 1 (Fig. 2*A*). Remarkably, the two pairs of residues [$I^{2i13(1018)}$ and $L^{2i16(1021)}$ vs. $F^{3i13(1565)}$ and $F^{3i16(1518)}$] are located in symmetric positions in the model. We therefore hypothesized that $I^{2i13(1018)}$ and $L^{2i16(1021)}$ could

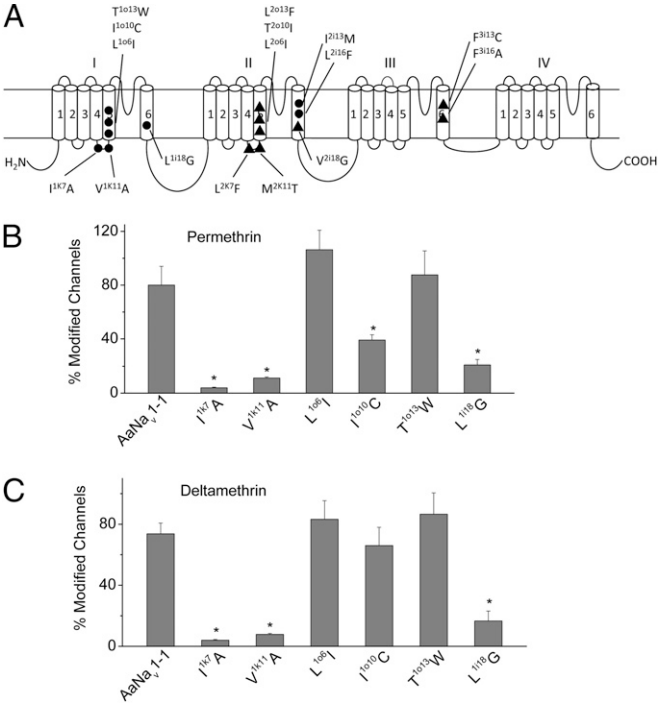

Fig. 2. Identification of a second pyrethroid-receptor site on the $AaNa_v1$–1 channel. (*A*) Topology of the sodium channel protein indicating key pyrethroid-sensing residues in site 1 (triangles) and site 2 (circles). Here we designate residues using the nomenclature that is universal for P-loop ion channels. A residue is labeled by the domain number (1–4, as I–IV in the topology), segment type (*k*, L45 linker; *i*, inner helix; *o*, outer helix), and the relative number of the residue in the segment (50). (*B* and *C*) Percentage of channel modification by permethrin (1 μM) (*B*) and deltamethrin (1 μM) (*C*). The number of oocytes for each mutant construct was >5. Error bars indicate mean ± SEM. Asterisks indicate significant differences from the $AaNa_v1$–1 channel as determined by using one-way analysis of variance with Scheffé's post hoc analysis ($P < 0.05$).

contribute to a second pyrethroid-receptor site. This site is formed by residues in IL45, IS5, and IIS6 (the IL45–IS5–IIS6 triangle), which would be analogous to site 1, formed by residues in IIL45, IIS5, and IIIS6 (the IIL45–IIS5–IIIS6 triangle).

To test the second binding site model, we conducted mutational analysis of the following additional residues in the predicted site 2: I^{1k7} and V^{1k11} in IL45 and L^{1o6}, I^{1o10}, and T^{1o13} in IS5 (Fig. 2*A*). The positions of these residues are analogous to those at site 1 that have been shown to confer pyrethroid resistance (Fig. 2*A*) (12, 14). In addition, we also included another residue, L^{1i18} in IS6, whose position is analogous to the kdr mutation $V^{2i18(1023)}G$ in IIS6 at site 1 that we have confirmed in this study. Three substitutions, $I^{1k7}A$, $V^{1k11}A$, and $T^{1o13}W$, altered the voltage dependence of activation and/or inactivation, whereas other substitutions did not (Table S2). In agreement with our prediction, $I^{1k7}A$, $V^{1k11}A$, and $L^{1i18}G$ reduced the sensitivity of the $AaNa_v1$–1 channel to PMT and DMT, whereas $I^{1o10}C$ reduced the sensitivity to PMT (Fig. 2 *B* and *C*). Interestingly, none of the three mutations in IS5 reduced the sensitivity to DMT and only one of them reduced the sensitivity to PMT (Fig. 2*B*). These results provide experimental evidence to support the existence of a second pyrethroid-receptor site in a pocket formed by the IL45–IS5–IIS6 triangle, but they also suggest that the precise architecture of site 1 and site 2 are not identical because, unlike site-1 mutations in IIS5, some of the corresponding mutations in IS5 did not have a strong effect on DMT or PMT action.

Refined Modeling of the Pyrethroid-Receptor Site 2 on the AaNa$_v$1–1 Channel. With the identification of residues I^{2i13}, L^{2i16}, I^{1k7}, V^{1k11}, and L^{1i18} as critical determinants for pyrethroid action at site 2, we used the Monte Carlo (MC) energy minimization method (MCM) to dock pyrethroids between the linker helix IL45 and transmembrane helices IS5, IS6, and IIS6. Preliminary docking of DMT in the K$_v$1.2-based model yielded two ensembles of binding modes in which the terminal CBr_2 and phenyl groups of DMT approached, respectively, either I^{1k7} and L^{1i18} (ensemble 1) or L^{1i18} and I^{1k7} (ensemble 2). Due to limited precision of homology models, energy alone could not be used to favor one of the ensembles. To resolve the problem, we searched for possible binding sites of tetramethylcyclopropane, the pyrethroid fingerprint model. Many random starting positions and orientations were generated and MC minimized. Calculations predicted that tetramethylcyclopropane fits a site between IL45, IS5, IS6, and IIS6 (Fig. 3*A*). The dimethylcyclopropane ring of DMT can approach this site in the first, but not the second ensemble. We further generated many initial placements of DMT and 1R-*cis*-permethrin (R-PMT), an active isomer of PMT (Fig. S3), between I^{1k7} and L^{1i18} of the open-channel model and searched for possible binding modes using many-stage MCM protocol (*SI Materials and Methods*). The predicted low-energy binding modes of DMT and R-PMT in the I/II interface are rather similar (Fig. 3 *B* and *C*). Most of the experimentally detected pyrethroid-sensing residues in IL45, IS6, and IIS6 form favorable contacts with the ligands. The CCl_2 or CBr_2 group binds between IL45 and IIS6, whereas the phenyl group binds between IS6 and IIS6, suggesting that the pyrethroid agonists increase the current by clamping the domain interface in its open state. Furthermore, the cyano group of deltamethrin directs toward the cytoplasm and binds in the I/II interface, where hydrophilic residues N^{2i20} and S^{1i29} are located. Further mutational and electrophysiological experiments involving different pyrethroids will be necessary to elaborate a more detailed model for the binding of type I and type II pyrethroids in sites 1 and 2.

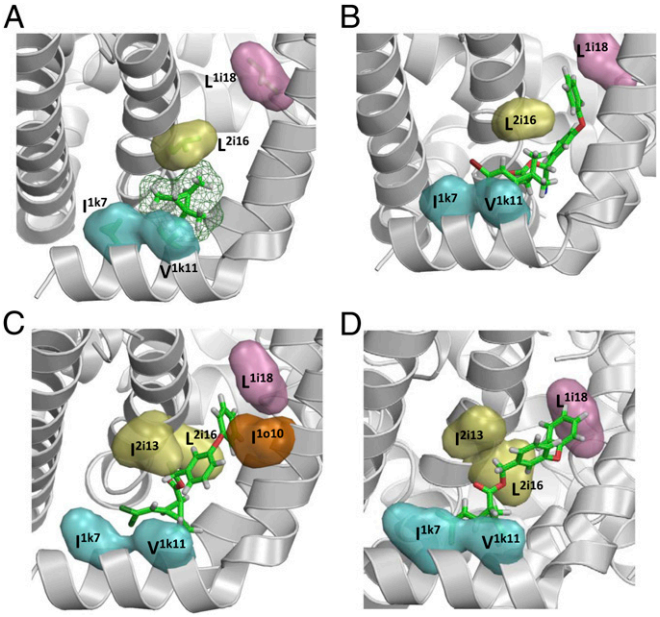

Fig. 3. Predicted complexes of the open AaNa$_v$1–1 channel (K$_v$1.2-based model) with tetramethylcyclopropane (*A*), deltamethrin (*B*), 1R-*cis*-permethrin (*C*), and 1S-*cis*-permethrin (*D*). Cyan, orange, pink, and yellow surfaces are side chains of pyrethroid-sensing residues in segments IL45, IS5, IS6, and IIS6, respectively. The halogen atoms of pyrethroids bind between IL45 and IIS6. The phenyl rings of deltamethrin and 1R-*cis*-permethrin (R-PMT) bind between IS6 and IIS6. The phenyl ring of the inactive 1S-*cis*-permethrin (S-PMT) forms weaker contacts with L^{1i18} and I^{2o13} compared with R-PMT.

In our models, the terminal aromatic group of deltamethrin binds between helices IS6 and IIS6, whereas the dibromoethenyl moiety binds between helices IIS6 and IL45. This orientation of the pyrethroid molecule ensures that the bulky rigid dimethylcyclopropane moiety fits between helices IL45, IS5, IS6, and IIS6, into a seemingly void space "below" the gating hinge (position *i14*). O'Reilly et al. (15) proposed a model in which the dimethylcyclopropane moiety of acrinathrin and bifenthrin binds "above" the gating hinge, in a region between two inner helices and the pore helix. In the X-ray structures of open potassium channels, contacts between alpha helices above the gating hinge are tighter than those below the gating hinge. Fitting the bulky dimethylcyclopropane moiety in a region of loose intraprotein contacts seems more likely than in a region of tight contacts.

In the completely extended conformation of DMT, the most distant heavy atoms (the terminal-phenyl *p*-carbon and a bromine) are ~14 Å apart. The most distant pyrethroid-sensing residues in both K$_v$1.2- and Na$_v$Ab-based homology models of the AaNa$_v$1–1 channel are I^{1k7} and L^{1i18}. C^{β} atoms of these residues are 18.8 and 21.4 Å apart in the respective models, suggesting that simultaneous interaction of DMT with both I^{1k7} and L^{1i18} is less likely in the closed channel than in the open channel. To test this, we MC minimized the Na$_v$Ab-based model with DMT constrained between I^{1k7} and L^{1i18}. In the low-energy binding modes of the completely extended conformations, DMT approached I^{1k7}, but not L^{1i18} (Fig. S4*A*).

Another striking feature of pyrethroids is their extreme stereospecificity for insecticidal activity: only certain stereoisomers are active (1). For example, among a total of four permethrin isomers, 1R-*cis* and 1R-*trans* isomers are active, whereas 1S-*cis* and 1S-*trans* isomers are inactive (1). Interestingly, although the inactive 1S-*cis* PMT (S-PMT) (Fig. S3) does not induce any tail current, it competitively inhibits the tail current induced by R-PMT, suggesting that S-PMT competes for the same binding sites with R-PMT (18, 36, 37). Consistent with these data, our modeling correctly predicted that S-PMT can bind to receptor site 2, but forms weaker contacts with L^{1i18} and I^{2i13} compared with R-PMT (Fig. 3*D*). The extreme lipophilicity of pyrethroids prevents evaluation of pyrethroid binding using conventional radioligand binding assays (12). As an alternative method, we have been using Schild analysis to determine the binding affinity of pyrethroids to sodium channels (18, 36, 37). In this study, we conducted Schild analysis of two additional site 2 mutant channels: I^{1k7}A and V^{1k11}A. The competitive replacement of R-PMT by S-PMT was significantly less efficient for I^{1k7}A and V^{1k11}A channels, compared with the wild-type channel (Fig. S5 and *SI Results*). Our results indicate that both I^{1k7} and V^{1k11} are involved in the binding of both S-PMT and R-PMT. Superposition of X-ray structures of the pH-gated bacterial potassium channel KcsA and the voltage-gated bacterial sodium channel Na$_v$Ab (38) indicates similar folding of the transmembrane region in the pore module, which supports our model. However, further refining of our model will be necessary when an X-ray structure of a eukaryotic sodium channel in the open state becomes available.

Contribution of Site 2 to Pyrethroid Selectivity on Insect vs. Mammalian Sodium Channels. A well-known property of pyrethroids is their differential action on insect vs. mammalian sodium channels (30, 39). Several mammalian sodium channel isoforms, such as rat Na$_v$1.2 (rNa$_v$1.2) and rat Na$_v$1.4 (rNa$_v$1.4), are virtually insensitive to pyrethroids in in vitro expression systems (27, 40, 41), which contributes to the favorable selective toxicity of pyrethroids (30, 39). Previously, the I^{2k11}M substitution, which corresponds to the super kdr mutation M^{2k11}T in IIL45 (site 1), was found to significantly enhance the sensitivity of rNa$_v$1.2 and rNa$_v$1.4 channels to pyrethroids (40, 41). Our discovery of site 2

prompted us to investigate the role of this site in mediating pyrethroid selectivity. We first explored a sequence alignment between insect and mammalian sodium channels (Fig. S6) to determine species-specific residues at site 2 that would explain the selectivity of pyrethroids between insect and mammalian sodium channels. Site 2 residues are highly conserved in insect sodium channels, but some of them are substituted in mammalian sodium channels (Fig. S6). Specifically, all insect sodium channels have V^{1k11} and I^{1o10}, whereas nine rat (also human) sodium channels have L^{1k11} and M^{1o10} at respective positions, except for T^{1o10} in $rNa_v1.8$ (Fig. S6). Furthermore, mutational analysis of site 2 residues in the cockroach sodium channel validates the importance of site 2 in pyrethroid sensitivity in another insect sodium channel (Figs. S7 and S8). Next, we performed amino acid substitution experiments by introducing insect site-2 residues into rat sodium channels. We found that the $M^{1o10}I$ substitution alone in $rNa_v1.2$ or $rNa_v1.4$ channels did not significantly increase the sensitivity of these channels to DTM (Fig. 4 *B* and *C*). The $L^{1k11}V$ substitution significantly increased the DMT sensitivity of $rNa_v1.4$, but not $rNa_v1.2$ (Fig. 4 *B* and *C*). Interestingly, the $M^{1o10}I/L^{1k11}V$ double mutations significantly enhanced the DMT sensitivity of both $rNa_v1.2$ and $rNa_v1.4$ channels (Fig. 4 *B* and *C*). Most remarkably, the $L^{1k11}V/M^{1o10}I/I^{2k11}M$ triple mutations produced channels that are much more sensitive to DTM than single- or double-mutant channels (Fig. 4 *B* and *C*). Taken together, these results demonstrate that site 2 is critically important for the selective action of pyrethroids on insect vs. mammalian sodium channels.

In the absence of X-ray structure of a eukaryotic sodium channel with bound pyrethroids, it is impossible to rule out the possibility that mutations of the residues in the proposed site 2 allosterically modify the binding of pyrethroids to the previously predicted site 1. However, several observations argue against such a possibility. First, the Hill analysis suggests that there is more than one pyrethroid binding site (19). Second, many residues in site 2 are rather far from the nearest residues in site 1. For example, beta carbons of L^{1i18} (site 2) and V^{2i18} (site 1) are as far as 13.3 Å apart. Third, the single site-1 model could not explain several kdr mutations, which can now be explained in view of the dual receptor-site model. Fourth, our computational model predicted several previously unknown pyrethroid-sensing residues in site 2. Indeed, subsequent experiments confirmed most of these predictions. Finally, site 2 contains pyrethroid-sensing residues that differ substantially between mammalian and insect channels (Fig. S6). A model with dual pyrethroid binding sites is therefore consistent with the well-known and fundamentally important selective toxicity of pyrethroids toward insects.

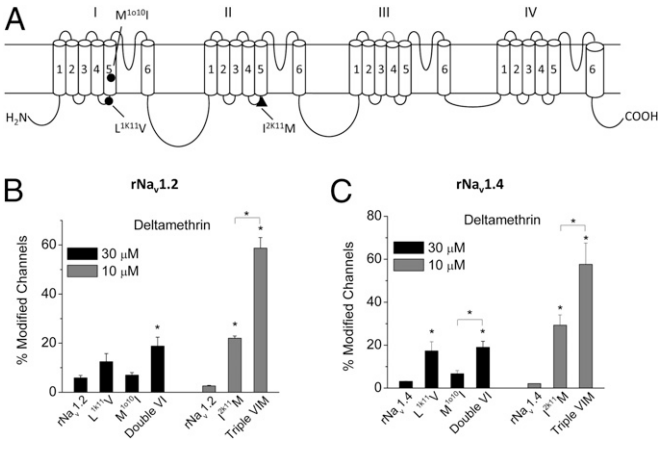

Fig. 4. Transferring $AaNa_v1–1$ site 2 residues into mammalian sodium channels enhances mammalian sodium channel sensitivity to deltamethrin. (*A*) Topology of the mammalian sodium channel indicating site 1 and site 2 residues substituted by respective $AaNa_v1–1$ channel residues. (*B* and *C*) Percentage of channel modification by deltamethrin of $rNa_v1.2$ (*B*) and $rNa_v1.4$ (*C*) and mutant channels. The number of oocytes for each mutant channel was >5. Error bars indicate mean ± SEM. Asterisks indicate significant differences as determined by using one-way analysis of variance with Scheffé's post hoc analysis ($P < 0.05$).

Conclusions and Implications

In this study, by establishing a *Xenopus* oocyte-based functional expression system for the *Ae. aegypti* $AaNa_v1–1$ sodium channel, we discovered a second putative pyrethroid-receptor site. Importantly, this second receptor site is likely universal in insect sodium channels, but is absent in mammalian sodium channels. Together with findings from a previous computer modeling study (15), our results suggest that simultaneous binding of pyrethroids to two receptor sites in a four-domain sodium channel is necessary to efficiently lock sodium channels in the open state and, thereby, to exert the highly insecticidal action. Specifically, trapping S4–S5 linkers and S6s of both domain I and domain II in the open conformation by pyrethroids is likely necessary to prevent deactivation. The discovery of dual pyrethroid-receptor sites is unprecedented for sodium channel neurotoxins and sets a unique paradigm for further elucidation of the action of pyrethroids at the molecular level. Furthermore, the finding from this study should have significant implications in guiding the development of strategies for monitoring and management of pyrethroid resistance in the control of mosquitoes and other medically and agriculturally important arthropod pests.

Materials and Methods

Cloning and Site-Directed Mutagenesis. Procedures for synthesis of first-strand cDNAs, PCR and cloning of the full-length $AaNa_v$ cDNA were similar to those described by Olson et al. (26). Site-directed mutagenesis was performed by PCR using specific primers and Pfu Turbo DNA polymerase (Agilent). Additional technical details are presented in *SI Materials and Methods*.

Expression of $AaNa_v$ Channels in *Xenopus* oocytes and Electrophysiology. Procedures for oocytes preparation and cRNA preparation and injection were identical to those described previously (18). Methods and data analysis for two-electrode voltage clamp recording of sodium currents, measurement of tail currents induced by pyrethroids and Schild analysis were identical to those previously described (18, 31). Results are reported as mean ± SEM. Statistical significance was determined by using one-way analysis of variance with Scheffé's post hoc analysis, and significant values were set at $P < 0.05$ as indicated in the figure legends. Additional technical details are presented in *SI Materials and Methods*.

Computer Modeling. Homology modeling and ligand docking were performed using the ZMM program, which minimizes the energy in the space of internal (generalized) coordinates (42, 43). Energy was calculated using the AMBER force field (44, 45). Atomic charges at ligands were calculated with the MOPAC program (46). Electrostatic energy was calculated using the environment- and distance-dependent dielectric function without desolvation energy (47). Bond angles were kept rigid in the protein, but were allowed to vary in the ligands. The energy optimization was performed by MCM protocol (48). All molecular images were created using PyMol.

Homology Modeling of the Mosquito Sodium Channel. The X-ray structures of the Na_vAb (6) and $K_v1.2$ (34) channels were used as templates, respectively, to build the closed and open conformations of the $AaNa_v1–1$ channel. $AaNa_v1–1$ was aligned with Na_vAb as in ref. 38. Extracellular turret regions in $AaNa_v1–1$ were truncated to match the lengths of the respective regions in Na_vAb. $AaNa_v1–1$ was aligned with $K_v1.2$ as in our previous models (49, 50). The outer pore of sodium channels does not fold like that of K_v channels. Therefore, in the $K_v1.2$-based model the P-loops were truncated at the most C-terminal position of the pore helices. This truncation does not affect ligand docking in the interface between IL45, IS5, IS6, and IIS6, which is too far from the outer pore. The homology models were built and MC minimized as described elsewhere (49). Docking of each pyrethroid ligand was performed in several stages as described in *SI Materials and Methods*.

ACKNOWLEDGMENTS. We thank Dr. Kris Silver for critical review of this manuscript and Dr. Bhupinder Khambay for permethrin isomers. We also would like to express our sincere gratitude to the late Professor Toshio Narahashi for his valuable input into this project. Computations were performed using the facilities of the Shared Hierarchical Academic Research Computing Network (SHARCNET, www.sharcnet.ca). This study was supported by Grant GM057440 (to K.D. and B.S.Z.) from National Institutes of Health and Grant MOP-53229 (to B.S.Z.) from the Natural Sciences and Engineering Research Council of Canada. S.Y.H. is a Howard Hughes Medical Institute–Gordon and Betty Moore Foundation Investigator.

1. Khambay BP, Jewess P (2005) Pyrethroids. *Comprehensive Molecular Insect Science*, eds Gilbert LI, Latrou K, Gill SS (Elsevier, Oxford, UK), Vol 6, pp 1–29.
2. World Health Organization (2007) *Insecticide-Treated Mosquito Nets: A WHO Position Statement* (WHO, Geneva).
3. World Health Organization (2009) *WHO Recommended Long-Lasting Insecticidal Mosquito Nets* (WHO, Geneva).
4. Doyle DA, et al. (1998) The structure of the potassium channel: Molecular basis of K+ conduction and selectivity. *Science* 280(5360):69–77.
5. Jiang Y, et al. (2002) The open pore conformation of potassium channels. *Nature* 417(6888):523–526.
6. Payandeh J, Scheuer T, Zheng N, Catterall WA (2011) The crystal structure of a voltage-gated sodium channel. *Nature* 475(7356):353–358.
7. Bloomquist JR (1996) Ion channels as targets for insecticides. *Annu Rev Entomol* 41(1): 163–190.
8. Narahashi T (1986) Mechanisms of action of pyretrhoids on sodium and calcium channel gating. *Neuropharmacology and Pesticide Action*, eds Ford MG, Usherwood PNR, Reay RC, Lunt GG (Ellis Horwood, Chichester, England), pp 36–60.
9. Narahashi T (1996) Neuronal ion channels as the target sites of insecticides. *Pharmacol Toxicol* 79(1):1–14.
10. Soderlund DM (2010) State-dependent modification of voltage-gated sodium channels by pyrethroids. *Pestic Biochem Physiol* 97(2):78–86.
11. Butler D (2011) Mosquitoes score in chemical war. *Nature* 475(7354):19.
12. Rinkevich FD, Du YZ, Dong K (2013) Diversity and convergence of sodium channel mutations involved in resistance to pyrethroids and DDT. *Pestic Biochem Physiol*, in press.
13. Davies TG, Field LM, Usherwood PN, Williamson MS (2007) DDT, pyrethrins, pyrethroids and insect sodium channels. *IUBMB Life* 59(3):151–162.
14. Soderlund D (2005) Sodium channels. *Comprehensive Molecular Insect Science*, eds Gilbert LI, Latrou K, Gill SS (Elsevier, New York), Vol 5, pp 1–24.
15. O'Reilly AO, et al. (2006) Modelling insecticide-binding sites in the voltage-gated sodium channel. *Biochem J* 396(2):255–263.
16. Du Y, et al. (2009) Identification of a cluster of residues in transmembrane segment 6 of domain III of the cockroach sodium channel essential for the action of pyrethroid insecticides. *Biochem J* 419(2):377–385.
17. Usherwood PNR, et al. (2007) Mutations in DIIS5 and the DIIS4-S5 linker of *Drosophila melanogaster* sodium channel define binding domains for pyrethroids and DDT. *FEBS Lett* 581(28):5485–5492.
18. Tan J, et al. (2005) Identification of amino acid residues in the insect sodium channel critical for pyrethroid binding. *Mol Pharmacol* 67(2):513–522.
19. Vais H, et al. (2000) Activation of Drosophila sodium channels promotes modification by deltamethrin. Reductions in affinity caused by knock-down resistance mutations. *J Gen Physiol* 115(3):305–318.
20. Dong K (2007) Insect sodium channels and insecticide resistance. *Invert Neurosci* 7(1): 17–30.
21. Jones CM, et al. (2012) Footprints of positive selection associated with a mutation (N1575Y) in the voltage-gated sodium channel of Anopheles gambiae. *Proc Natl Acad Sci USA* 109(17):6614–6619.
22. Li T, et al. (2012) Multiple mutations and mutation combinations in the sodium channel of permethrin resistant mosquitoes, *Culex quinquefasciatus. Sci Rep* 2:781.
23. Xu Q, et al. (2012) Evolutionary adaptation of the amino acid and codon usage of the mosquito sodium channel following insecticide selection in the field mosquitoes. *PLoS ONE* 7(10):e47609.
24. Feng G, Deák P, Chopra M, Hall LM (1995) Cloning and functional analysis of TipE, a novel membrane protein that enhances Drosophila para sodium channel function. *Cell* 82(6):1001–1011.
25. Warmke JW, et al. (1997) Functional expression of Drosophila para sodium channels. Modulation by the membrane protein TipE and toxin pharmacology. *J Gen Physiol* 110(2):119–133.
26. Olson RO, Liu ZQ, Nomura Y, Song WZ, Dong K (2008) Molecular and functional characterization of voltage-gated sodium channel variants from *Drosophila melanogaster*. *Insect Biochem Mol Biol* 38(5):604–610.
27. Smith TJ, Soderlund DM (1998) Action of the pyrethroid insecticide cypermethrin on rat brain IIa sodium channels expressed in xenopus oocytes. *Neurotoxicology* 19(6): 823–832.
28. Song W, Liu Z, Tan J, Nomura Y, Dong K (2004) RNA editing generates tissue-specific sodium channels with distinct gating properties. *J Biol Chem* 279(31):32554–32561.
29. Narahashi T (1988) Molecular and cellular approaches to neurotoxicology: past, present and future. *Neurotox '88: Molecular Basis of Drug and Pesticide Action*, ed Lunt GG (Elsevier, New York), pp 563–582.
30. Soderlund DM (2012) Molecular mechanisms of pyrethroid insecticide neurotoxicity: Recent advances. *Arch Toxicol* 86(2):165–181.
31. Tatebayashi H, Narahashi T (1994) Differential mechanism of action of the pyrethroid tetramethrin on tetrodotoxin-sensitive and tetrodotoxin-resistant sodium channels. *J Pharmacol Exp Ther* 270(2):595–603.
32. Burton MJ, et al. (2011) Differential resistance of insect sodium channels with kdr mutations to deltamethrin, permethrin and DDT. *Insect Biochem Mol Biol* 41(9): 723–732.
33. Hu Z, Du Y, Nomura Y, Dong K (2011) A sodium channel mutation identified in *Aedes aegypti* selectively reduces cockroach sodium channel sensitivity to type I, but not type II pyrethroids. *Insect Biochem Mol Biol* 41(1):9–13.
34. Long SB, Campbell EB, Mackinnon R (2005) Crystal structure of a mammalian voltage-dependent Shaker family K+ channel. *Science* 309(5736):897–903.
35. Zhorov BS, Tikhonov DB (2004) Potassium, sodium, calcium and glutamate-gated channels: Pore architecture and ligand action. *J Neurochem* 88(4):782–799.
36. Du Y, et al. (2010) A negative charge in transmembrane segment 1 of domain II of the cockroach sodium channel is critical for channel gating and action of pyrethroid insecticides. *Toxicol Appl Pharmacol* 247(1):53–59.
37. Lund AE, Narahashi T (1982) Dose-dependent interaction of the pyrethroid isomers with sodium channels of squid axon membranes. *Neurotoxicology* 3(1):11–24.
38. Tikhonov DB, Zhorov BS (2012) Architecture and pore block of eukaryotic voltage-gated sodium channels in view of NavAb bacterial sodium channel structure. *Mol Pharmacol* 82(1):97–104.
39. Narahashi T, Zhao X, Ikeda T, Nagata K, Yeh JZ (2007) Differential actions of insecticides on target sites: Basis for selective toxicity. *Hum Exp Toxicol* 26(4):361–366.
40. Vais H, et al. (2000) A single amino acid change makes a rat neuronal sodium channel highly sensitive to pyrethroid insecticides. *FEBS Lett* 470(2):135–138.
41. Wang SY, Barile M, Wang GK (2001) A phenylalanine residue at segment D3-S6 in Nav1.4 voltage-gated Na(+) channels is critical for pyrethroid action. *Mol Pharmacol* 60(3):620–628.
42. Zhorov BS (1981) Vector method for calculating derivatives of the energy deformation of valence angles and torsion energy of complex molecules according to generalized coordinates. *J Struct Chem* 22:4–8.
43. Zhorov BS (1983) Vector method for calculating derivatives of the energy deformation of valence angles and torsion energy of complex molecules according to generalized coordinates. *J Struct Chem* 23:649–655.
44. Weiner SJ, et al. (1984) A new force field for molecular mechanical simulation of nucleic acids and proteins. *J Am Chem Soc* 106(3):765–784.
45. Weiner SJ, Kollman PA, Nguyen DT, Case DA (2004) An all atom force field for simulations of proteins and nucleic acids. *J Comput Chem* 7(2):230–252.
46. Dewar MJS, Zoebisch EG, Healy EF, Stewart JJP (1985) Development and use of quantum mechanical molecular models. 76. AM1: A new general purpose quantum mechanical molecular model. *J Am Chem Soc* 107(13):3902–3909.
47. Garden DP, Zhorov BS (2010) Docking flexible ligands in proteins with a solvent exposure- and distance-dependent dielectric function. *J Comput Aided Mol Des* 24(2): 91–105.
48. Li Z, Scheraga HA (1987) Monte Carlo-minimization approach to the multiple-minima problem in protein folding. *Proc Natl Acad Sci USA* 84(19):6611–6615.
49. Du Y, Garden DP, Wang LX, Zhorov BS, Dong K (2011) Identification of new batrachotoxin-sensing residues in segment IIIS6 of the sodium channel. *J Biol Chem* 286(15):13151–13160.
50. Du Y, Garden D, Khambay B, Zhorov BS, Dong K (2011) Batrachotoxin, pyrethroids, and BTG 502 share overlapping binding sites on insect sodium channels. *Mol Pharmacol* 80(3):426–433.